Induced potential of a dust particle in a collisional radio-frequency sheath

Lu-Jing Hou and You-Nian Wang*
State Key Lab of Materials Modification by Beams, Department of Physics, Dalian University of Technology, Dalian 116023, China

Z. L. Mišković
Department of Applied Mathematics, University of Waterloo, Waterloo, Ontario, Canada N2L 3G1
(Received 14 January 2003; published 24 July 2003)

A hydrodynamic model is established to study the interactions of a dust particle with a radio-frequency (rf) sheath, taking into account the influence of the spatial inhomogeneity of the (rf) sheath, as well as the influence of the ion-neutral collisions. Numerical results are obtained for the charge on the dust particle and for the spatial distribution of the induced potential around this particle, based on a self-consistent modeling of the sheath parameters such as the sheath electric field, the ion velocity, and the ion and electron densities. The induced potential exhibits the familiar oscillatory structure of a wake potential, which is, however, strongly damped due to the collisional effects. The spatial inhomogeneity of the rf sheath gives rise to a further damping of the induced potential, as well as to a reduction of the oscillations at large distances from the dust particle.

DOI: 10.1103/PhysRevE.68.016410 PACS number(s): 52.40.Hf, 52.25.Vy, 52.35.Fp

I. INTRODUCTION

It has been observed in a series of experiments [1–4] that the highly charged dust particles in the radio-frequency (rf) plasma sheath assemble themselves into ordered Coulomb crystal structures such as the body-centered-cubic, face-centered-cubic, and simple hexagonal structures. Those experiments have stimulated extensive studies of many interesting phenomena in dusty plasmas and the related fields such as the phase transitions [5–7] of the dust crystals, wave propagations in the dust crystals [8–12], the charging process of a dust particle [13–17], and the nonlinear interactions between the charged microparticles and rf sheaths [18–21]. Furthermore, it is believed that the plasma crystals may provide a unique model system where the phase transitions and the lattice defects could be observed by means of very simple devices, or even by naked eyes, owing to its fast response property and an easy observability.

The precise mechanism of the dust crystal formation is still an open question, although it has been studied extensively, both theoretically and experimentally [22–39], during the past several years. The trouble lies in the explanation of the interactions among the alike charged particles; namely, it is well known that, in a typical experiment with the plasma crystal, the dust particles immersed in the plasma sheath collect thousands of electrons on their surfaces. So, one may expect that the Coulomb repulsions among these negatively charged particles will be very strong. Nevertheless, the ordered structures observed in the dust crystals, especially the alignments of the particles in the direction perpendicular to the electrode, indicate that there must exist some attractive interactions among those particles. By now, several theoretical models have been proposed to explain such kind of interactions among the dust particles. In particular, the theory of the wake potential [22–31], which is based on the collective effects in a plasma with the ion flow in the direction perpendicular to the electrode, can provide a qualitative explanation for the formation of vertical arrangements in the dust crystal; namely, it has been demonstrated that, due to the ion flows, an oscillatory wake potential appears ''behind'' a static test dust particle, so that the other dust particles may be trapped in the potential minima. Such an attraction among the highly charged dust particles can overcome the Coulomb repulsion and may provide the mechanism for the dust crystal formation. For example, numerical simulations [28] based on the wake theory have successfully reproduced the results of the experiments [32,33] in which the vertically aligned dust particles were manipulated by the laser tweezers, revealing some kind of an asymmetry in the attractive interactions among the particles.

It appears that all theoretical studies of the wake potential to date have used the common assumptions that the dust particles are placed in a homogeneous background plasma with a constant ion flow and a zero electric field, while neglecting the collisional effects between the ions and neutral particles. In typical experimental conditions [1–6,18–20], however, it is well known that the dust particles often levitate near the boundary of the sheath regions, where the ion density and the electron density are inhomogeneous, the sheath electric field is not zero, and the ion velocity also increases due to the acceleration in the sheath electric field. Thus, one expects that the spatial inhomogeneities of the rf sheath may exert a great influence on the wake potential. In addition, the discharge pressures in the experiments with the dust crystals range typically from several Pa to about 100 Pa. In that case, the ion-neutral collisional effects in the sheath will be significant and may give rise to a spatial damping of the wake potential.

In this paper, we present a model of the wake potential, taking into account both the spatial inhomogeneity of the sheath and the ion-neutral collisional effects. In Sec. II, a self-consistent model of the rf sheath field is described by collisional ion dynamics, which gives the time-averaged sheath field, the charge densities, and the ion velocity. Based on such sheath model, we determine in Sec. III the charge

*Email address: ynwang@dlut.edu.cn

and the levitating position of the dust particle in the sheath. In Sec. IV, we use the linear hydrodynamic equations to derive a general expression of the wake potential for the dust particle levitating in the inhomogeneous sheath. Finally, we give a short summary in Sec. V.

II. SHEATH MODEL

We consider that a rf-bias power is applied to a flat electrode inside a plasma, so that a rf sheath is formed near the electrode surface, allowing us to adopt a one-dimensional configuration along the z axis oriented into the plasma, with the electrode placed at $z=0$. Since the rf is much larger than the ion plasma frequency, we can neglect all time-dependent terms in the ion fluid equations. On the other hand, the effects of the ion-neutral collisions on the rf sheath dynamics should be considered, since the experiments [1–6,18–20] have been performed at quite high pressures. Therefore, the spatiotemporal variations of the quantities, such as the ion density $n_{i0}(z,t)$, the ion drift velocity $u_{i0}(z,t)$, the electric field $E_0(z,t)$, and the potential $\Phi_0(z,t)$, are determined by the ion continuity equation [41]

$$\frac{d(n_{i0}u_{i0})}{dz}=0, \tag{1}$$

the ion momentum balance

$$m_i u_{i0}\frac{du_{i0}}{dz}=eE_0-\frac{\pi m_i}{2\lambda_i}u_{i0}^2, \tag{2}$$

and the field equations

$$\frac{dE_0}{dz}=4\pi e(n_{i0}-n_{e0}),$$

$$\frac{d\Phi_0}{dz}=-E_0, \tag{3}$$

where m_i and e are the ion mass and the elementary charge, respectively. The second term on the right-hand side of Eq. (2) comes from the charge-exchange collisions, with λ_i being the mean collisional free path [42]. In Eq. (3), n_{e0} is the electron density, given by the Boltzmann relation

$$n_{e0}(z,t)=n_0\exp\left(\frac{e\Phi_0(z,t)}{T_e}\right), \tag{4}$$

where n_0 is the plasma density and T_e is the electron temperature.

In order to solve Eqs. (1)–(4), appropriate boundary conditions at the plasma-sheath interface must be chosen. Compared to the direct-current sheath, the rf sheath boundary conditions are quite complex and the boundary may oscillate in a rf cycle. Thus, we assume that at the plasma-sheath boundary, placed at $z=d_s(t)$, the ion density should be equal to the electron density, $n_{i0}(d_s,t)=n_{e0}(d_s,t)=n_0$. In addition, we also assume that the ions enter the sheath with a velocity equal to $u_0=u_B(1+\pi\lambda_D/\lambda_i)^{-1/2}$, where $u_B=(T_e/m_i)^{1/2}$ is the Bohm velocity and $\lambda_D=(T_e/4\pi n_0 e^2)^{1/2}$ is the electron Debye length in the bulk plasma. Finally, we assume that the potential at the sheath edge is approximately 0, $\Phi_0(d_s,t)=0$, and takes the value of the potential at the electrode ($z=0$) to be $\Phi_0(0,t)=V_e(t)$, where $V_e(t)$ is the instantaneous potential drop across the sheath.

In order to determine, in a self-consistent manner, the relationship between the instantaneous voltage $V_e(t)$ and the instantaneous sheath thickness $d_s(t)$, we adopt the approach developed by Edelberg and Aydil [41], based on the following current-balance equation at the electrode of area A:

$$A\left[eu_i(0,t)n_i(0,t)-\frac{eu_e n_0}{4}\exp\left(\frac{eV_e(t)}{k_B T_e}\right)-\frac{\varepsilon_0}{d_s(t)}\frac{dV_e(t)}{dt}\right]$$
$$=I_{\max}\sin(2\pi ft). \tag{5}$$

Here, the first two terms on the left-hand side are the ion current and the electron current incident on the electrode, respectively, the third term is the capacitive displacement current due to temporal variation of the voltage at the electrode, whereas the term on the right-hand side is the applied rf-bias current with the amplitude $I_{\max}$ and the frequency f. Note that, in Eq. (5), $u_e=\sqrt{8T_e/\pi m_e}$ is the mean velocity of an electron with mass m_e. Equations (1)–(5) can be solved numerically by means of the fourth-order Runge-Kutta method. The solution procedure requires an initial guess for $d_s(t)$, which allows numerical integration of Eq. (5) to obtain the potential drop $V_e(t)$. Using the above boundary conditions, then Eqs. (1)–(4) are integrated over the interval $[0,V_e(t)]$, which gives a new value for $d_s(t)$. Such an iterative procedure is repeated until the time-dependent solutions converge to a self-consistent periodic steady state. Note that the relation between the rf-bias current amplitude $I_{\max}$ and the average rf bias power to the electrode is given by

$$\langle P_{rf}\rangle=\frac{1}{\tau}\int_0^\tau dt\, I_{\max}\sin(2\pi ft)\, V_e(t), \tag{6}$$

where $\tau=1/f$ is the rf period. Thus, by solving the above equations numerically, we first obtain the instantaneous spatial distributions of the ion density $n_{i0}(z,t)$, the electron density $n_{e0}(z,t)$, the ion velocity $u_{i0}(z,t)$, the electric field $E_0(z,t)$, and the potential $\Phi_0(z,t)$ in the sheath, and then perform the time averaging, indicated in Eq. (6), in order to obtain the corresponding equilibrium quantities, i.e., $n_{i0}(z)=\langle n_{i0}(z,t)\rangle$, $n_{e0}(z)=\langle n_{e0}(z,t)\rangle$, and $u_{i0}(z)=\langle u_{i0}(z,t)\rangle$, $\Phi_0(z)=\langle\Phi_0(z,t)\rangle$, $E_0(z)=\langle E_0(z,t)\rangle$.

In the following calculations, we take an argon discharge as an example, with the plasma density $n_0=1\times10^9$ cm^{-3}, the electron temperature $T_e=3.0$ eV, the rf power 2.0 W, and the discharge pressure p ranging from 10 Pa to 50, as typical parameters used in such kind of experiments. Then, Figs. 1(a)–(c) show the spatial variations of the average electric field, the average ion and electron densities, and the average ion velocity in the sheath, for several discharge pressures. We notice from the figures that, for a given discharge pressure, both the intensity of the sheath field and the ion velocity increase with increasing distance from the plasma

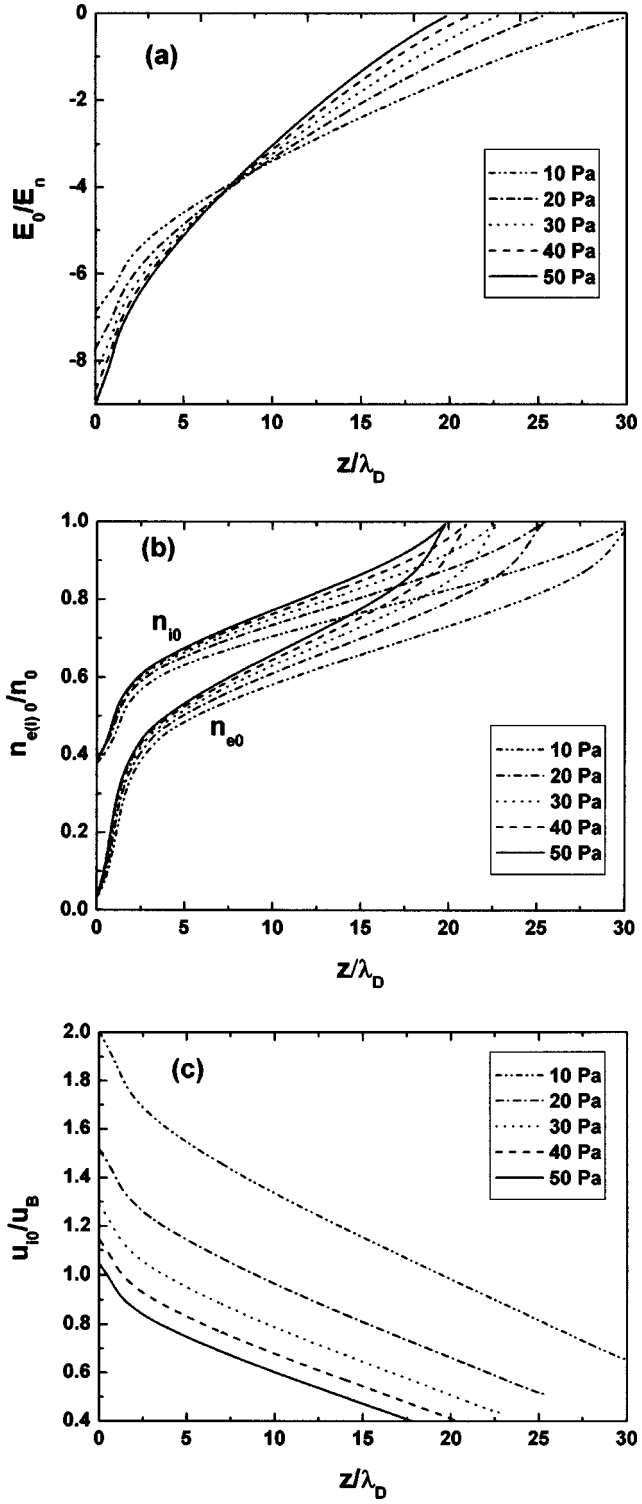

FIG. 1. The dependence of the sheath quantities on the perpendicular distance z to the electrode: (a) average electric field $E_0(z)$, (b) average ion density $n_{i0}(z)$ and electron density $n_{e0}(z)$, and (c) average ion velocity $u_{i0}(z)$, for several discharge pressures. Here, λ_D is the electron Debye length in the plasma and $E_n = T_e/(e\lambda_D)$.

boundary, while, in the same time, the ion and the electron densities decrease. In addition, one can see that, with increasing discharge pressures, the sheath thickness is reduced and the ion velocity decreases in magnitude, while the charged-particle densities increase, due to the collisional effects. In particular, the electron density is lower than the corresponding ion density within the sheath. Therefore, we may expect that the spatial inhomogeneity of the sheath, as well as the collisional effects, will affect the structure of the wake potential of dust particles in the rf sheath.

III. LEVITATING AND CHARGING

We consider now a dust particle with the mass m_d trapped in the rf sheath. As it has been seen in the preceding sections, the electric field, the ion density, and the ion velocity within the rf sheath exhibit spatial and temporal variations. In general, the time scale of the dust particle motion in the sheath is much longer than the rf period. Therefore, we can assume in the following that the particle responds to the time-averaged sheath quantities, $E_0(z)$, $n_{i0}(z)$, $n_{e0}(z)$, and $u_{i0}(z)$, rather than to their instantaneous values. Then, the levitating position of the particle z_d can be determined by the force balance

$$m_d g = E_0(z_d) Q(z_d) - F_i(z_d), \tag{7}$$

where g is the gravitational acceleration, $Q(z_d)$ is the particle charge at the position z_d, and $F_i(z_d)$ is the ion flow drag force [43].

The usual approach for determining the dust particle charge is to assume that the particle is an electrically floating, spherical capacitor with a capacitance $C = 4\pi\varepsilon_0 a$ [20,40], where a is its radius. So the equilibrium charge on the particle can be written as

$$Q(z_d) = C\Phi_p(z_d), \tag{8}$$

where Φ_p is the floating potential of the dust, defined relative to the local plasma potential. The floating potential is determined by the balance of the electron and ion currents collected by the particle, i.e., $I_e + I_i = 0$. We use here the well-known orbital motion limited (OML) theory [20,40] to express the ion and the electron charging currents, respectively, as follows:

$$I_i(\Phi_p, z_d) = n_0 e \pi a^2 \left(\frac{T_e}{m_i}\right)^{1/2} \left[1 - 2\frac{e\Phi_p}{T_e}\left(\frac{u_B}{u_{i0}(z_d)}\right)^2\right], \tag{9}$$

and

$$I_e(\Phi_p, z_d) = -n_{e0}(z_d) e \pi a^2 \left(\frac{8T_e}{\pi m_e}\right)^{1/2} \exp\left(\frac{e\Phi_p}{T_e}\right). \tag{10}$$

The dust particle will acquire an equilibrium floating potential Φ_p when the net current goes to 0. Here, we should stress that the floating potential is related to the electron density $n_{e0}(z)$ and the ion velocity $u_{i0}(z)$ in the sheath.

As an example, we consider in this paper a dust particle with radius $a = 3.5 \times 10^{-4}$ cm and mass density $\rho_m = 1.05$ g/cm^3. We determine the levitating position z_d and the equilibrium charge $Q(z_d)$ of the particle from Eqs. (7)–(10). Using the plasma parameters given in the preceding section, we show in Fig. 2 the spatial dependence of the

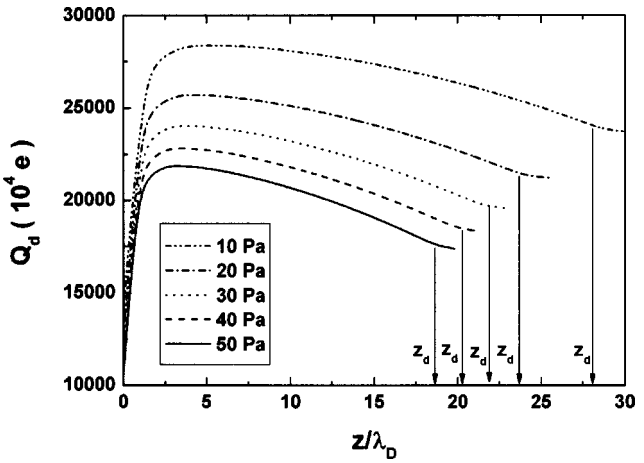

FIG. 2. The charges on the dust particle in the sheath vs the perpendicular distance z to the electrode, for several discharge pressures. The arrows indicate the levitating positions z_d of the dust particle in the sheath. λ_D is the electron Debye length in the plasma.

charge $Q(z)$ within the sheath for several discharge pressures. One can see that the levitating positions of the particles are almost near the sheath boundary and that the equilibrium charge $Q(z_d)$ decreases with increasing discharge pressure.

IV. WAKE POTENTIAL

The presence of a dust particle in the sheath gives rise to perturbations in the electron density and the ion density around the particle. In that case, the total scalar potential Φ in the sheath is determined by the Poisson equation

$$\nabla^2\Phi(\mathbf{r}) = -4\pi[en_i(\mathbf{r}) - en_e(\mathbf{r}) - Q_d\delta(\mathbf{r}-\mathbf{r}_d)], \quad (11)$$

where $\mathbf{r}_d$ is the particle equilibrium position, while $n_i(\mathbf{r})$ and $n_e(\mathbf{r})$ are the total ion density distribution and the total electron density distribution, respectively. Within the framework of the hydrodynamics, the ion motion can be described by the continuity equation

$$\boldsymbol{\nabla}\cdot[n_i(\mathbf{r})\mathbf{u}_i(\mathbf{r})] = 0, \quad (12)$$

and the momentum equation,

$$\mathbf{u}_i(\mathbf{r})\cdot\boldsymbol{\nabla}\mathbf{u}_i(\mathbf{r}) = -\frac{Z_i e}{m_i}\boldsymbol{\nabla}\Phi(\mathbf{r}) - \nu\mathbf{u}_i(\mathbf{r}). \quad (13)$$

Here, $\mathbf{u}_i$ is the ion velocity field and $\nu = \pi u_{i0}/2\lambda_i$ is the collisional frequency. The electron density is still determined by the Boltzmann relation, or the equation

$$\boldsymbol{\nabla}n_e(\mathbf{r}) = \frac{en_e}{T_e}\boldsymbol{\nabla}\Phi(\mathbf{r}). \quad (14)$$

The system of Eqs. (11)–(14) constitute a set of self-consistent nonlinear equations, which can only be solved numerically, in general. As is usually done in the linear dielectric-response theory [22–29], we linearize the above equations by assuming $n_i(\mathbf{r}) = n_{i0} + n_{i1}(\mathbf{r})$, $\mathbf{u}_i(\mathbf{r}) = u_{i0}\mathbf{e}_z + \mathbf{u}_{i1}(\mathbf{r})$, $n_e(\mathbf{r}) = n_{e0} + n_{e1}(\mathbf{r})$, $\mathbf{E}(\mathbf{r}) = \mathbf{E}_0(z) + \mathbf{E}_1(\mathbf{r})$, and $\Phi(\mathbf{r}) = \Phi_0(z) + \Phi_1(\mathbf{r})$, where $n_{i0}(z)$, $u_{i0}(z)$, $n_{e0}(z)$, $\mathbf{E}_0(z)$, and $\Phi_0(z)$ are the equilibrium quantities determined by the sheath model of Sec. II, while $n_{i1}(\mathbf{r})$, $\mathbf{u}_{i1}(\mathbf{r})$, $n_{e1}(\mathbf{r})$, $\mathbf{E}_1(\mathbf{r})$, and $\Phi_1(\mathbf{r})$ are the perturbed quantities. In comparison with the perturbed quantities, the spatial variation of the equilibrium quantities is rather slow, so that we resort to a local approximation in solving the linearized Eqs. (11)–(14). In this approximation, we apply the three-dimensional Fourier transform only on the perturbed quantities that exhibit rapid dependence on the spatial coordinates $\mathbf{r}$, while the slow variation of the equilibrium quantities allows us to consider them parametrically dependent on the z coordinate. This enables us to obtain, using simple algebraiac operations, the Fourier transform of the potential in the mixed form, $\tilde{\Phi}_1(\mathbf{k};z)$, where $\mathbf{k}$ is the Fourier variable dual to $\mathbf{r}$. Then, the inverse Fourier transform, $\Phi_1(\mathbf{r}) = (2\pi)^{-3}\int d^3\mathbf{k}\, e^{i\mathbf{k}\cdot\mathbf{r}}\tilde{\Phi}_1(\mathbf{k};z)$, restores the z dependence as a fast variation superimposed on the slow variation of the equilibrium sheath quantities. In particular, we obtain the perturbed potential, relative to the equilibrium position of the dust particle $\mathbf{r}_d$, as follows

$$\Phi_1(\mathbf{r}) = -\frac{Q_d}{2\pi^2}\int\frac{d\mathbf{k}}{k^2}\frac{e^{i\mathbf{k}\cdot(\mathbf{r}-\mathbf{r}_d)}}{\varepsilon(k,-\mathbf{k}\cdot\mathbf{u}_{i0})}, \quad (15)$$

where $\varepsilon(k,-\mathbf{k}\cdot\mathbf{u}_{i0})$ is the dielectric function of the plasma,

$$\begin{aligned}\varepsilon(k,\omega) = 1 &- \frac{\omega_{sh}^2(k^2-\omega^2/u_{i0}^2)}{k^2(\omega-iu_{i0}')(\omega+i\nu)} \\ &- \frac{\omega_{sh}^2\omega^2/u_{i0}^2}{k^2(\omega-iu_{i0}')(\omega+i\nu-iu_{i0}')} \\ &+ \frac{i\omega_{sh}^2 n_{i0}'\omega/n_{i0}u_{i0}}{k^2(\omega-iu_{i0}')(\omega+i\nu-iu_{i0}')} \\ &+ \frac{1}{(k\lambda_{sh})^2}\frac{1}{1-ieE_0\omega/T_e u_{i0}k^2}. \end{aligned} \quad (16)$$

Here, $\omega = -\mathbf{k}\cdot\mathbf{u}_{i0} = k_z u_{i0}$, $u_{i0}' = du_{i0}/dz$, $n_{i0}' = dn_{i0}/dz$, whereas $\lambda_{sh} = (T_e/4\pi n_{e0}e^2)^{1/2}$ is the electron Debye length in the sheath, and $\omega_{sh} = (4\pi n_{i0}e^2/m_i)^{1/2}$ is the ion plasma frequency in the sheath. Note that, within the local approximation, the equilibrium quantities in Eqs. (15) and (16), n_{i0}, n_{e0}, E_0, and u_{i0}, and the derivatives n_{i0}' and u_{i0}' are all (slow) functions of z. It is easy to show that, for a homogeneous background plasma, i.e., when $u_{i0}' = 0$, $n_{i0}' = 0$, and $E_0 = 0$, Eq. (16) reduces to the well-known form [22–26]

$$\varepsilon(k,\omega) = 1 + \frac{1}{(k\lambda_D)^2} - \frac{\omega_{pi}^2}{\omega(\omega+i\nu)}, \quad (17)$$

where λ_D and $\omega_{pi} = (4\pi n_0 e^2/m_i)^{1/2}$ are the Debye length and the ion plasma frequency, respectively, both in the bulk plasma.

In general, the perturbed potential can be separated into two parts, viz.,

$$\Phi_1(\rho,z)=\frac{-Q_d}{|\mathbf{r}-\mathbf{r}_d|}+\Phi_{ind}(\rho,z), \tag{18}$$

where the first part is the bare Coulomb potential of the dust particle and the second part is the induced potential of the particle. In the cylindrical coordinates, $\mathbf{r}=(\boldsymbol{\rho},z)$, the induced potential can be written as

$$\Phi_{ind}(\rho,z)=\frac{-\Phi_d}{\pi u_{i0}}\int_0^{k_{\max}}\frac{dk}{k}\int_{-ku_{i0}}^{ku_{i0}}d\omega J_0((\rho-\rho_d)\sqrt{k^2-\omega^2/u_{i0}^2})\Pi(k,\omega,z), \tag{19}$$

where J_0 is the zeroth-order Bessel function and

$$\Pi(k,\omega,z)=\mathrm{Re}[\varepsilon^{-1}(k,\omega)-1]\cos[\omega(z-z_d)/u_{i0}]-\mathrm{Im}[\varepsilon^{-1}(k,\omega)-1]\sin[\omega(z-z_d)/u_{i0}]. \tag{20}$$

Here, we have replaced the upper limit ∞ in the k integral by a cutoff constant $k_{\max}$ to avoid the integration divergence when $k\to\infty$. Generally, the characteristic length of the plasma polarization is about the order of the Debye length λ_D, so it is reasonable to choose the constant approximately as $k_{\max}=1/\lambda_D$ [22–29]. Finally, it should be mentioned that, after performing the Fourier back-transform, all the equilibrium quantities remain dependent on z.

In Fig. 3, we show the dependence of the perturbed potential Φ_1 on the dimensionless longitudinal distance $(z-z_d)/\lambda_D$ for a fixed transversal distance $\rho-\rho_d=1.8\lambda_D$, with Fig. 3(a) corresponding to the case of a spatially inhomogeneous sheath and Fig. 3(b) to the homogeneous case. The two sets of curves in Figs. 3(a) and 3(b) are shown for several values of the discharge pressures, selected according to the typical experimental conditions [4,5] of plasma crystal. One may notice from both Figs. 3(a) and 3(b) that, as the discharge pressure increases, the magnitude of the wake potential decreases significantly due to the increasing role of the ion-neutral collisions. Actually, there are two reasons for the drop of the magnitude of the induced potential. One is that the charge Q_d on the dust particle decreases with increasing discharge pressure, while the other is that the polarization of the medium becomes weaker due to the collisional effect. We mention that, if the discharge pressure is low enough, for example, $p=1$ Pa, the oscillations in the potential become more pronounced, so that the wake potential in the homogeneous case becomes very similar to our previous results [28,29], where both the collisional effects and the spatial inhomogeneity were ignored.

When comparing Fig. 3(a) with Fig. 3(b), we also find that, for a given discharge pressure, the oscillatory structures of the wake potential in the inhomogeneous case are rather different from those in the homogeneous case. Considering the short distances from the dust particle, the magnitude of the wake potential in the inhomogeneous case appears to be significantly reduced compared to the homogeneous case.

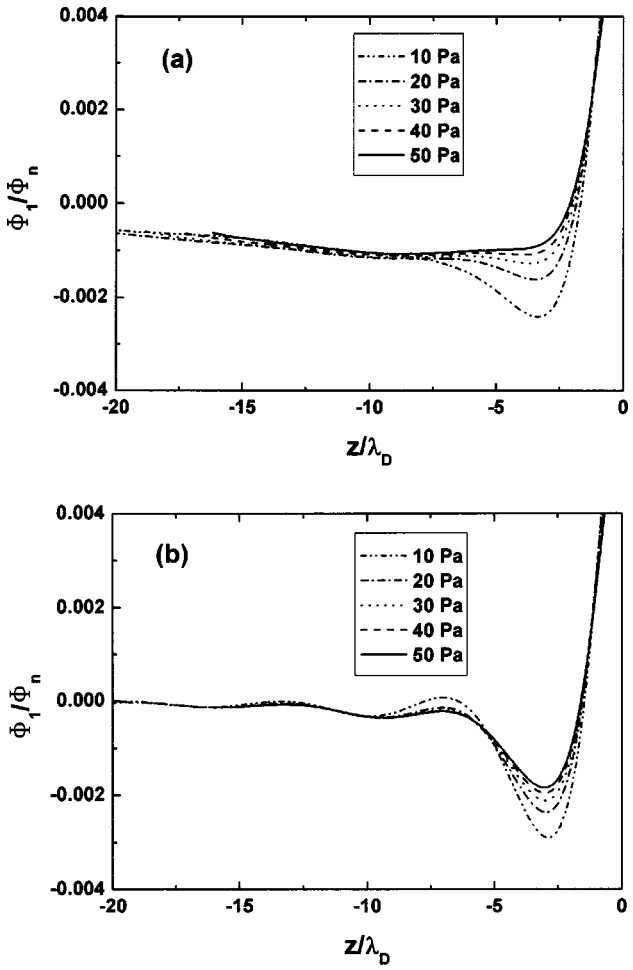

FIG. 3. The perturbed potential Φ_1 of the dust particle as a function of the longitudinal distance $(z-z_d)/\lambda_D$, with the transversal distance $\rho-\rho_d=1.8\lambda_D$, for several discharge pressures: (a) potential in the (inhomogeneous) sheath and (b) potential in the homogeneous plasma. Here, z_d is the levitating position of the dust particle in the sheath, λ_D is the electron Debye length in the plasma, and $\Phi_n=T_e/e$.

More interestingly, for long distances from the dust particle, say, past the first minima in the wake, it appears that the oscillations are practically absent in the inhomogeneous case, while they still persist in the homogeneous case. Finally, while the induced potential vanishes at very long distances behind the dust particle in the homogeneous case, we observe a long tail in the inhomogeneous case. These tendencies can be seen more clearly in Figs. 4 and 5, which display the dependence of the wake potential on both $(\rho-\rho_d)/\lambda_D$ and $(z-z_d)/\lambda_D$ in the inhomogeneous and homogeneous cases, respectively, for three different discharge pressures. The inhomogeneous case is apparently again characterized by a more damped magnitude of the induced potential, the reduced oscillations, and the long tails, when compared with the homogeneous case, which can be rationalized as follows. Since the electron density $n_{e0}(z)$ in the sheath is smaller than the plasma density n_0, see Fig. 1(b), the electron Debye length in the sheath will be larger than that in the homogeneous case, whereas it is well known [22–24] that the mag-

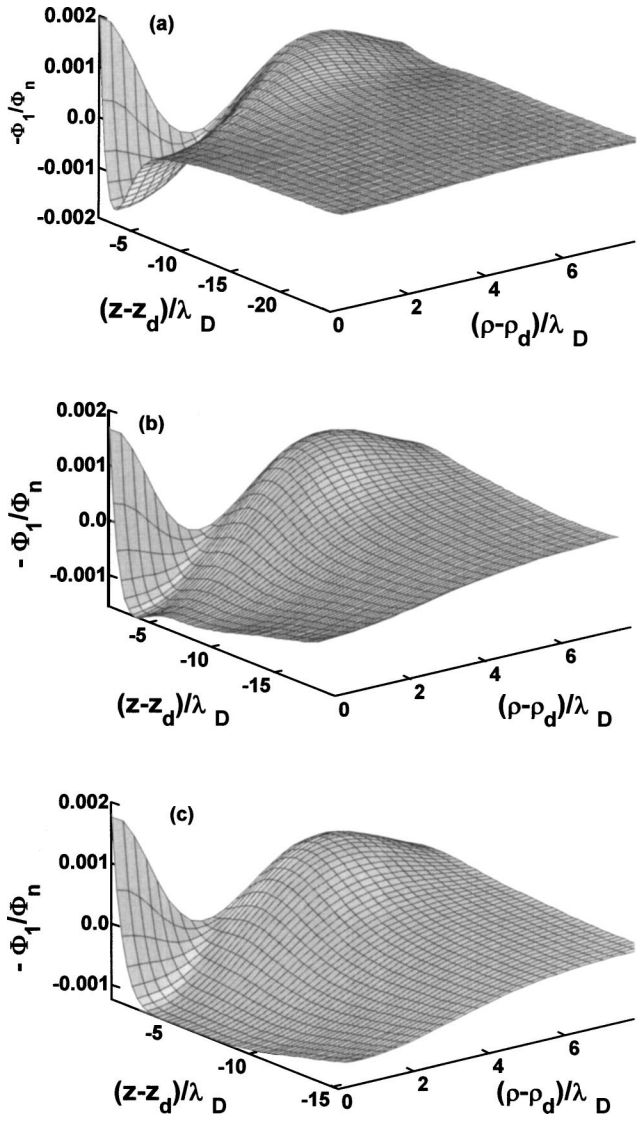

FIG. 4. The profiles of the perturbed potential Φ_1 of the dust particle in the (inhomogeneous) sheath for three discharge pressures: (a) $p=10$ Pa, (b) $p=30$ Pa, and (c) $p=50$ Pa. Here, λ_D is the electron Debye length in the plasma and $\Phi_n=T_e/e$.

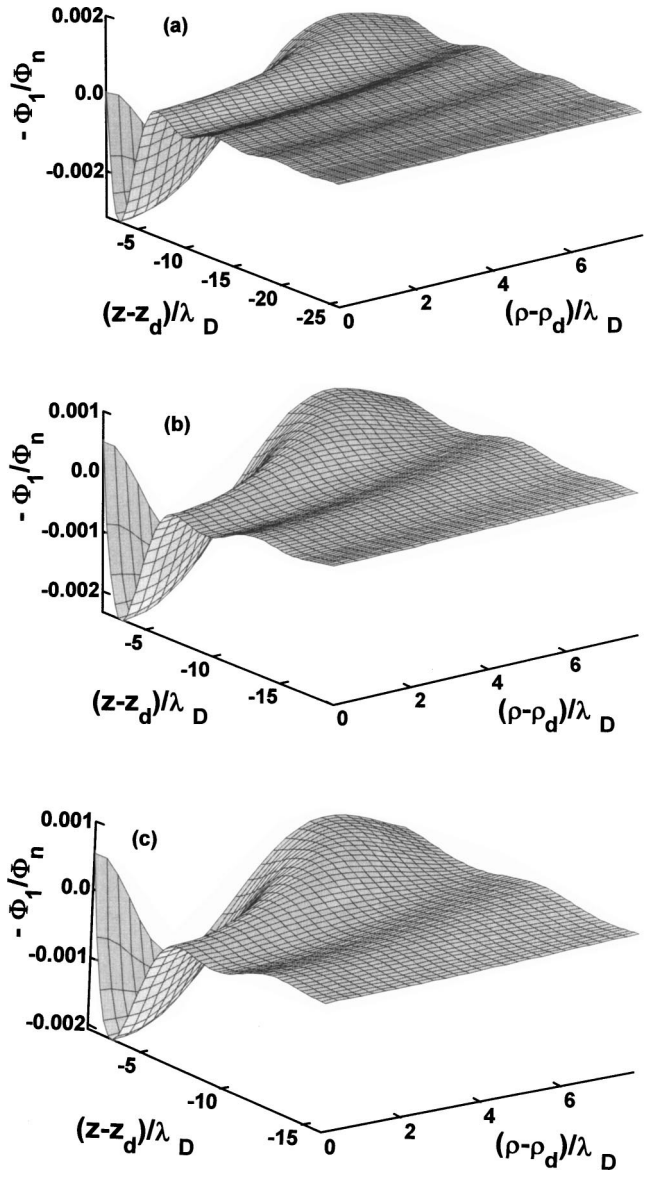

FIG. 5. The profiles of the perturbed potential Φ_1 of the dust particle in the homogeneous plasma for three discharge pressures: (a) $p=10$ Pa, (b) $p=30$ Pa, and (c) $p=50$ Pa. Here, λ_D is the electron Debye length in the plasma and $\Phi_n=T_e/e$.

nitude of the oscillating wake potential is approximately inversely proportional to the electron Debye length. On the other hand, the increase in the ion velocity in the sheath also results in the increase in the Mach number $M=u_{i0}(z)/u_B$, which can further increase the wavelength of the oscillatory potential, virtually converting the oscillations into long tails. So, we can conclude that the characteristics of the wake potential in the sheath are strongly influenced by the variations in the ion oscillating frequency, the electron Debye length, and the Mach number.

V. SUMMARY

In this paper, we have studied theoretically the interactions of a dust particle with the rf plasma sheath going beyond the theoretical framework of the homogeneous collisionless plasma background. A one-dimensional dynamical model of a collisional rf sheath has been developed to determine the influence of the discharge pressure on the spatial distributions of some physical quantities in the sheath, such as the average electric field, the average ion density, the average electron density, and the average ion velocity. With such sheath model, we have further determined the levitating position and the charge of the dust particle in the sheath. It has been found that the particle levitates near the sheath boundary and its charge decreases with increasing discharge pressure. Finally, based on the model of the linearized fluid dynamics, we have used the local approximation to evaluate the induced potential of the dust particle in the sheath, which exhibits characteristic oscillations of the wake potential. Nu-

merical results show that, as the discharge pressure is raised, the collisional effects become increasingly important, giving rise to a reduction of the magnitude of the wake potential. The results also show that the spatial inhomogeneity of the sheath further dampens the potential and, moreover, rectifies the oscillations in the wake for large distances from the dust particle. These surprisingly strong effects give rise to the qualitative properties of the wake model, with possibly important implications for studying the dust crystal formation, which warrant further investigation. In particular, the prominent role of the inhomogeneity of the rf plasma sheath should be studied by extending the linearized fluid dynamics model beyond the local approximation.

ACKNOWLEDGMENTS

This work was jointly supported by the National Natural Science Foundation of China (Grant Nos. 19975008 and 10275009) and by MOEC (Ministry of Education, China) Grant for Cross-Century Excellent Scholar (Y.N.W.). Support from the Natural Sciences and Engineering Research Council of Canada is also acknowledged (Z.L.M.).

[1] Y. Hayashi and K. Tachibana, Jpn. J. Appl. Phys., Part 2 **33**, L804 (1994).
[2] J.H. Chu and I. Lin, Phys. Rev. Lett. **72**, 4009 (1994).
[3] H. Thomas, G.E. Morfill, V. Demmel, J. Goree, B. Feuerbacher, and D. Mohlmann, Phys. Rev. Lett. **73**, 652 (1994).
[4] A. Melzer, T. Trottenberg, and A. Piel, Phys. Lett. A **191**, 301 (1994).
[5] H.M. Thomas and G.E. Morfill, Nature (London) **379**, 806 (1996).
[6] H.M. Thomas and G.E. Morfill, J. Vac. Sci. Technol. A **14**, 501 (1996).
[7] V.A. Schweigert, I.V. Schweigert, A. Melzer, A. Homann, and A. Pei, Phys. Rev. Lett. **80**, 5345 (1998).
[8] R. Singh and M.P. Bora, Phys. Plasmas **7**, 2335 (2000).
[9] M. Zuzic, H.M. Thomas, and G.E. Morfill, J. Vac. Sci. Technol. A **14**, 496 (1996).
[10] A. Barkan, N. D' Angelo, and R.L. Merlino, Planet. Space Sci. **44**, 239 (1996).
[11] M. Rosenberg, Planet. Space Sci. **44**, 229 (1993).
[12] R.L. Merlino, IEEE Trans. Plasma Sci. **25**, 60 (1997).
[13] E. Thomas, Jr and M. Watson, Phys. Plasmas **7**, 3194 (2000).
[14] J.W. Manweiler, T.P. Armstrong, and T.E. Cravens, J. Plasma Phys. **63**, 269 (2000).
[15] G. Lapenta, Phys. Plasmas **6**, 1442 (1999).
[16] G. Lapenta, Phys. Rev. Lett. **75**, 4409 (1995).
[17] A.A. Mamun, P.K. Shukla, and T. Farid, Phys. Plasmas **7**, 2329 (2000).
[18] H. Schollmeyer, A. Melzer, A. Homann, and A. Piel, Phys. Plasmas **6**, 2693 (1999).
[19] A.V. Ivlev, R. Sutterlin, V. Steinberg, M. Zuzic, and G. Morfill, Phys. Rev. Lett. **85**, 4060 (2000).
[20] C. Zafiu, A. Melzer, and A. Piel, Phys. Rev. E **63**, 066403 (2001).
[21] Y.N. Wang, L.J. Hou, and X. Wang, Phys. Rev. Lett. **89**, 155001 (2002)
[22] S.V. Vladimirov and M. Nambu, Phys. Rev. E **52**, R2172 (1995).
[23] S.V. Vladimirov and O. Ishihara, Phys. Plasmas **3**, 444 (1996).
[24] O. Ishihara and S.V. Vladimirov, Phys. Plasmas **4**, 69 (1997).
[25] O. Ishihara, S.V. Vladimirov, and N.F. Cramer, Phys. Rev. E **61**, 7246 (2000).
[26] M. Lampe, G. Joyce, and G. Ganguli, Phys. Plasmas **7**, 3851 (2000).
[27] B.S. Xie, K.F. He, and Z.Q. Huang, Phys. Lett. A **253**, 83 (1999).
[28] L.J. Hou, Y.N. Wang, and Z.L. Mišković, Phys. Lett. A **292**, 129 (2001).
[29] L.J. Hou, Y.N. Wang, and Z.L. Mišković, Phys. Rev. E **64**, 046406 (2001).
[30] G. Lapenta, Phys. Rev. E **62**, 1175 (2000).
[31] G. Lapenta, Phys. Plasmas **6**, 1442 (1999).
[32] K. Takahashi, T. Oishi, K.I. Shimomai, Y. Hayashi, and S. Nishino, Phys. Rev. E **58**, 7805 (1998).
[33] A. Melzer, V.A. Schweigert, and A. Piel, Phys. Rev. Lett. **83**, 3194 (1999).
[34] D. Winske, W. Daughton, D.S. Lemons, and M.S. Murillo, Phys. Plasmas **7**, 2320 (2000).
[35] U. Konopka, G.E. Morfill, and L. Ratke, Phys. Rev. Lett. **84**, 891 (2000).
[36] S. Nunomura, N. Ohno, and S. Takamura, Phys. Plasmas **5**, 3517 (1998).
[37] F. Melandso and J. Goree, J. Vac. Sci. Technol. A **14**, 511 (1996).
[38] D.S. Lemons, M.S. Murillo, W. Daughton, and D. Winske, Phys. Plasmas **7**, 2306 (2000).
[39] P.K. Shukla and N.N. Rao, Phys. Plasmas **3**, 1770 (1996).
[40] T. Nitter, Plasma Sources Sci. Technol. **5**, 93 (1996).
[41] E.A. Edelberg and E.S. Aydil, J. Appl. Phys. **86**, 4799 (1999).
[42] H.T. Qiu, Y.N. Wang, and T.C. Ma, J. Appl. Phys. **90**, 5884 (2001).
[43] M.S. Barnes, J.H. Keller, J.C. Forster, J.A. O'Neill, and D.K. Coultas, Phys. Rev. Lett. **68**, 313 (1992).